J Physiol 585.1 (2007) pp 117–134

Synaptic heterogeneity between mouse paracapsular intercalated neurons of the amygdala

Raffaella Geracitano[1], Walter A. Kaufmann[2], Gabor Szabo[3], Francesco Ferraguti[2] and Marco Capogna[1]

[1]*MRC, Anatomical Neuropharmacology Unit, Oxford OX1 3TH, UK*
[2]*Department of Pharmacology, Innsbruck Medical University, A-6020 Innsbruck, Austria*
[3]*Laboratory of Molecular Biology and Genetics, Institute of Experimental Medicine, 1083 Budapest, Hungary*

GABAergic medial paracapsular intercalated (Imp) neurons of amygdala are thought of as playing a central role in fear learning and extinction. We report here that the synaptic network formed by these neurons exhibits distinct short-term plastic synaptic responses. The success rate of synaptic events evoked at a frequency range of 0.1–10 Hz varied dramatically between different connected cell pairs. Upon enhancing the frequency of stimulation, the success rate increased, decreased or remained constant, in a similar number of cell pairs. Such synaptic heterogeneity resulted in inhibition of the firing of the postsynaptic neurons with different efficacies. Moreover, we found that the different synaptic weights were mainly determined by diversity in presynaptic release probabilities rather than postsynaptic changes. Sequential paired recording experiments demonstrated that the same presynaptic neuron established the same type of synaptic connections with different postsynaptic neurons, suggesting the absence of target-cell specificity. Conversely, the same postsynaptic neuron was contacted by different types of synaptic connections formed by different presynaptic neurons. A detailed anatomical analysis of the recorded neurons revealed discrete and unexpected peculiarities in the dendritic and axonal patterns of different cell pairs. In contrast, several intrinsic electrophysiological responses were homogeneous among neurons, and synaptic failure counts were not affected by presynaptic cannabinoid 1 or $GABA_B$ receptors. We propose that the heterogeneous functional connectivity of Imp neurons, demonstrated by this study, is required to maintain the stability of firing patterns which is critical for the computational role of the amygdala in fear learning and extinction.

(Received 6 August 2007; accepted after revision 1 October 2007; first published online 4 October 2007)
Corresponding author M. Capogna: MRC Anatomical Neuropharmacology Unit, Mansfield Road, Oxford OX1 3TH, UK. Email: marco.capogna@pharm.ox.ac.uk

Synaptic transmission in the mammalian brain is unreliable; the probability of release at an individual synapse is in the range of 0.1–0.9 (Dobrunz & Stevens, 1997), so that failures and postsynaptic events result from the activity of the presynaptic neuron. The reliability of synaptic transmission in the central nervous system (CNS) is further affected by the fact that the amplitude of the unitary postsynaptic responses varies from trial to trial (Bekkers *et al.* 1990; Larkman *et al.* 1991). Is there any computational advantage to synaptic unreliability? At the level of a single synapse, the lack of reliability offers a large dynamic range so that an increase of release probability, generated for example by action potentials occurring at high frequency, enhances synaptic efficacy (Abbott & Nelson, 2000; Thomson, 2000; Zucker & Regehr, 2002). At the population level, one can imagine that synapses with heterogeneous synaptic strengths can contribute to maintain stability of firing rates in the cellular network they create. Indeed, a theoretical model in which the strengths of inhibitory synapses in a central pattern-generating circuit is dependent on activity-dependent plasticity has been proposed (Soto-Trevino *et al.* 2001).

We have investigated this issue in mouse paracapsular intercalated (Ip) (Alheid *et al.* 1994) neurons of the amygdala, which are GABAergic neurons surrounding the deep amygdaloid nuclei (Millhouse, 1986; Nitecka & Ben-Ari, 1987; McDonald & Augustine, 1993; Pare & Smith, 1993*a*). We specifically focused on Ip cells with the soma in the intermediate capsule (the medial subdivision, Imp), as they have been proposed to act as an inhibitory gate between the basolateral (BL) and the central (Ce) nuclei of the amygdala under cortical control (Royer *et al.* 1999, 2000; Royer & Pare,

This paper has online supplemental material.

DOI: 10.1113/jphysiol.2007.142570

2002; Berretta *et al.* 2005). Current views on amygdala function assign a paramount role to Imp neurons in inhibiting the expression of conditioned fear and in the storage of extinction memory (Pare *et al.* 2004). Characteristically, Imp neurons appear to exhibit striking features. When recorded *in vivo*, they display remarkably high discharge rates (Collins & Pare, 1999) compared to projection neurons of BL or Ce nuclei (Pare & Gaudreau, 1996). Moreover, the average synaptic weight remains constant when activity-dependent potentiation or depression occurs at different sites of the dendritic tree of an Imp neuron (Royer & Pare, 2003). In addition, they receive the densest afferents from the mesencephalic dopaminergic system (Fuxe *et al.* 2003). Interestingly, dopamine, which enhances fear learning and expression (Borowski & Kokkinidis, 1998), selectively hyperpolarizes and depresses the excitability of Ip cells while exciting other interneurons of amygdala, resulting in a disinhibition of the BL and Ce nuclei (Marowsky *et al.* 2005).

Based on the prominent role that inhibitory circuits intrinsic to the amygdala appears to have for fear learning and extinction (Pare *et al.* 2004), it is paramount to progress our understanding of the synaptic dynamics that entail Ip neuronal networks. Therefore, we have performed paired recordings between anatomically identified Imp neurons, and found that these neurons are connected with variable synaptic weights depending on the frequency of the activity of the presynaptic neuron. We have further defined groups of synaptically coupled Imp neurons based on the aspects of the dendritic and axonal patterns of the recorded neurons.

Methods

Preparation of acute slices

All procedures involving animals were performed according to methods approved by the UK Home Office and The Animals (Scientific Procedures) Act 1986. Every effort was made to minimize the number of animals used and their suffering. We used glutamate decarboxylase 65 (GAD65)–green fluorescent protein (GFP) transgenic mice and details on the generation of these mice have been previously published (Lopez-Bendito *et al.* 2004). Acute coronal slices were prepared from 17.2 ± 0.3-day-old mice. Animals were deeply anaesthetized with isoflurane in oxygenated air and then decapitated. The brain was rapidly removed and placed in semi-frozen sucrose ACSF cutting solution containing (mM): 75 sucrose, 87 NaCl, 2.5 KCl, 0.5 $CaCl_2$, 7 $MgCl_2$, 1.25 NaH_2PO_4, 25 $NaHCO_3$, 25 glucose, pH 7.3 and bubbled with 95% O_2–5% CO_2. Slices (330 μm) were cut (Leica VT 1000S, Leica Microsystems GmbH, Nussloch, Germany) and transferred to a nylon mesh where they were maintained in a chamber containing sucrose ACSF at 37°C for 30 min before returning to room temperature (24–26°C) for another 30 min. During this 1 h time period, sucrose ACSF was substituted with normal ACSF at a rate of 1–2 ml min^{-1}.

Electrophysiology and analysis

Acute slices were secured under a nylon mesh, submerged and superfused (at 1–2 ml min^{-1} and at 34 ± 1°C) with ACSF, containing (mM) 130 NaCl, 3.5 KCl, 2.5 $CaCl_2$, 1.5 $MgSO_4$, 1.25 NaH_2PO_4, 24 $NaHCO_3$, 10 glucose (all from VWR International), pH 7.4 (bubbled with 95% O_2–5% CO_2), in a 2 ml chamber mounted on the stage of an upright microscope (Axioskop or Axioskop 2 FS, Zeiss, Jena, Germany). Slices were visualized with a 10×, 0.3 NA or a 40×, 0.8 NA (Zeiss) water-immersion objective coupled with infrared and differential interference contrast (DIC) optics linked to a video camera (Newvicon C2400, Hamamatsu, Hamamatsu City, Japan), and a 100 W mercury vapour short-arc lamp (N HBO 103, Zeiss) connected to an epifluorescence system to visualize the GFP-expressing neurons (see online supplemental material, Supplemental Fig. 1). The labelled neurons helped initially to identify the intermediate capsule in the slices. However, in the majority of experiments, a 60×, 0.9 NA objective (Olympus, Great Western Industrial Park, Middlesex, UK) was used and the neurons were identified online with infrared and DIC optics by their location in the slice without the help of the epifluorescence illumination (see Supplemental Fig. 1). In this way, an unbiased sample of Imp neurons was collected (Lopez-Bendito *et al.* 2004). Somatic whole cell patch clamp recordings were performed from visually identified cells using borosilicate glass capillaries (GC120F, 1.2 mm o.d., Clarke Electromedical Instruments, Reading, UK, 4–6 MΩ), pulled on a DMZ puller (Zeitz-instrumente GmbH, Munich, Germany) and filled with a filtered intracellular solution consisting of (mM): 126 potassium gluconate, 4 KCl, 4 Mg-ATP, 0.3 Na-GTP, 10 Na_2-phosphocreatine, 10 Hepes and 0.5% w/v biocytin (all from Sigma-Aldrich Co. Ltd, Poole, UK), osmolarity 270–280 mosmol l^{-1} without biocytin, pH 7.3 with KOH. Biocytin was added to allow *post hoc* visualization of the recorded neurons. A CsCl-based intracellular solution was employed to record spontaneous inhibitory synaptic currents consisting of (mM): 140 CsCl, 4 NaCl, 1 Mg-Cl_2, 0.4 Na-GTP, 4 Na_2-ATP, 10 Hepes, 0.05 EGTA and 0.5% w/v biocytin (all from Sigma-Aldrich Co. Ltd, Poole, UK), osmolarity 270–280 mosmol l^{-1} without biocytin, pH 7.3 with CsOH. Cells were only accepted if the initial seal resistance was greater than 1 GΩ. The series resistance (R_s) was compensated online by 50–70% in voltage clamp mode to reduce voltage errors, and cells were only accepted for analysis if the initial R_s did not change by more than 25% throughout the recording period. Throughout the text, the membrane potential for the current clamp recordings has been corrected for an experimentally determined liquid junction potential of −12 mV. All electrophysiological signals were amplified (10 mV pA^{-1}, EPC9/2 amplifier HEKA Electronik, Lambrecht, Germany, Pulse software), filtered at 2.9 kHz and digitized at 5 or 10 kHz, and the amplifier was controlled from a personal computer (Power Mac G4, Macintosh or Systemax PC, AMD Athlon Processor, Systemax Systems) running the Pulse data acquisition and analysis program (HEKA).

Currents/voltages were acquired online with Pulse software and analysed offline with IGOR Pro 5 software (Wavemetrics Inc, Lake Oswego, OR, USA). Presynaptic action currents (voltage clamp) or action potentials (current clamp) were evoked by a voltage step bringing the potential up to 20 mV for 3 ms and a current step of 900 pA and 3 ms duration, respectively. The peak amplitude, latency, 20–80% rise time, decay time (fitted with a single exponential), area, jitter and failure of unitary events were analysed with a user-defined program in IGOR. A trace was classified as a failure by using the following criteria: when the peak amplitude was less than three times the s.d. of the average of the baseline noise, when the onset of the events was five times bigger than the s.d. of the onset of the average of events, or when the difference between the end and the onset of the event was smaller than 10 ms. Failures and the other synaptic parameters were also checked by manual analysis in IGOR. The failure rate was calculated as the number of failures divided by the number of trials (50 sweeps). The paired-pulse ratio, including failures, was calculated as the mean peak amplitude of the response to the second stimulus divided by the mean peak amplitude of the response to the first stimulus (30 sweeps). When failures were excluded the paired-pulse ratio of the successes only was computed as the potency ratio. The analysis of spontaneous synaptic currents was performed offline with MiniAnalysis (Synaptosoft, Decatur, GA, USA), as previously reported (Capogna *et al.* 2003). In current clamp experiments, the frequency of the action potentials was measured as the number of action potentials occurring over 30 s. The frequency of action potentials was also calculated for an 80 ms time window starting from the peak of a presynaptic action potential (referred as the onset of the unitary IPSP) and for an 80 ms time window starting from 600 ms after the onset of the unitary IPSP (number of sweeps used = 50). The input resistance (R_{in}) was calculated from the slope of a line fitted to the subthreshold range on a plot of the injected current *versus* the steady-state membrane voltage when a family of hyperpolarizing and depolarizing current injections were applied. The apparent membrane time constant (τ) was calculated by fitting a single exponential to the response of the cell to a current injection of −50 pA in current clamp mode. Membrane capacitance was calculated as τ/R_{in}. To study the kinetics of action potentials, a depolarizing current step (3 ms, 500–800 pA) was applied and action potential half-width, peak amplitude and membrane after-hyperpolarization (AHP) were measured from the initial point of the raising phase of the action potential by a user-defined program in IGOR. The sag ratio was calculated from the membrane potential at the end of a 1 s hyperpolarizing pulse divided by the largest membrane potential change observed in response to a current step of −200/−250 pA. The adaptation index was calculated as the ratio between the first and last interspike intervals evoked by a 1 s depolarizing current pulse. The maximal firing rate was the number of action potentials elicited by a strong (250–500 pA) depolarizing current pulse.

Histological processing of recorded cells

After electrophysiological recordings, slices were sandwiched between two filter papers (cellulose nitrate membrane filters, 0.45 μm, Whatman International Ltd, Maidstone, UK) and immersed in a fixative composed of 4% paraformaldehyde and ∼0.2% picric acid in phosphate buffer (PB; 0.1 m, pH 7.4) for at least 24 h. For some slices 0.05% glutaraldehyde (Agar Scientific Ltd, Essex, UK) was included in the fixative. Then, slices were embedded in a block of gelatin and re-sectioned into 50–60 μm slices with a Leica VT 1000S vibroslicer. Sections were washed in Tris-buffered saline (TBS; 0.9% NaCl, 0.05 m Tris, pH 7.4) and incubated overnight at 4°C in a 1 : 100 solution of avidin–biotinylated horseradish peroxidase complex (Vector Laboratories, Burlingame, CA, USA) in TBS + 0.1% Triton X-100 (VWR International Lutterworth, Leicestershire, UK). Sections were further washed in TBS and Tris buffer (TB; 0.05 m, pH 7.4) before incubation in 0.5 mg ml^{-1} diaminobenzidine (DAB, Sigma) in TB. Hydrogen peroxide (0.003%) was added to start the peroxidase reaction, which was carried out in TB. Sections were rinsed in TB, then PB, and subsequently mounted on gelatin coated slides and left to air-dry overnight. Sections were then hydrated, counterstained with 0.5% cresyl violet acetate (Sigma), dehydrated in graded ethanol (EtOH; 50%, 70%, 90%, 95% and 100% × 2), immersed in n-butyl acetate (Merck Sharp & Dohme, Hertfordshire, UK) and permanently mounted on slides. Neurons were reconstructed using a drawing tube. A 40× objective was used to draw the cells. The great majority of recorded pairs ($n = 83$) were identified as Imp neurons because their somata and/or dendrites were located in the intermediate capsule (these pairs are referred to as rigorously identified in Supplemental Table 1). A minority of pairs were classified as tentatively identified ($n = 5$) when, due to large spillage of biocytin, several somata were filled although most, but not all, of the labelled neurons were confined to the intermediate capsule together with staining in afferent and efferent areas of the Imp. For some rigorously identified pairs full anatomical characterization has not been possible because of the presence of more than two somata in the intermediate capsule which precluded thorough assessment of the axonal projections, or due to the loss of some of the sections of the slice. Immunofluorescence experiments were carried out according to previously published procedures (Ferraguti *et al.* 2004). Briefly, free-floating sections were preincubated for 1 h in blocking solution, composed of 20% normal goat serum (NGS), 0.1% Triton X-100 in TBS. The sections were then incubated in primary antibodies in combination or alone, made up in TBS, 0.1% Triton X-100, and 1% NGS for approximately 48 h (4°C). Primary antibodies used in this study were rabbit polyclonal anti-GFP (diluted 1 : 2500, Molecular Probes, no. A11122), and mouse monoclonal anti-enkephalin (diluted 1 : 250, Sigma, no. MAB350). Biocytin was visualized with streptavidin-7-amino-4-methylcoumarin (AMCA) (1 : 1000; Vector). After extensive washes in TBS, sections were incubated overnight (4°C) with a mixture of appropriate secondary antibodies: donkey anti-rabbit Alexa 488 (1 : 1000; Molecular Probes), and donkey anti-mouse Cy3™ (1 : 400; Jackson Immunoresearch Europe Ltd, Newmarket, UK). Sections were then washed and mounted onto gelatin-coated slides in Vectashield (Vector). Immunofluorescence was studied using a Zeiss Axioplan2 microscope with epifluorescence illumination. Images were analysed and displayed using the Openlab software (version 3.1.4; Improvision, Coventry, UK). Brightness and contrast were adjusted for the whole frame and no part of a frame was modified in any way.

Statistical tests

The success rate of events, as opposed to failures, was plotted *versus* frequency of stimulation and fitted by a non-linear regression analysis using a logarithmic equation: $y(x) = y_0 + a\ln(x)$, where y is the event rate, y_0 is the event rate when the frequency is equal to 1 Hz, a is the regression coefficient and x is the frequency of stimulation. Data throughout the text are presented as means ± s.e.m. Non-parametric two-tailed tests (Kruskal–Wallis with Dunn's *post hoc* comparison, Mann–Whitney U, Wilcoxon signed ranks, Chi square test) were used as indicated throughout the text. Where the number of observations was ≤ 5 we used the paired t test due to the low power of the Wilcoxon signed ranks test for small samples.

Chemicals and drugs

All drugs were superfused to the slices through the bath solution. Salts used for the patch pipette solution and ACSF were obtained from either VWR International or Sigma. Drugs (Tocris Cookson Inc., Avonmouth, UK) were added at the following concentrations: SR 95531 hydrobromide (gabazine, 2 μM), AM251 (10 μM), CGP55845 (5 μM), WIN55212–2 (5 μM), baclofen (3 μM).

Results

Synapses between Imp neurons have heterogeneous strengths

We have performed paired recordings between visually identified Imp neurons in slices obtained from GAD65–GFP mice (Lopez-Bendito *et al.* 2004), in which the green fluorescent protein is expressed under the control of the GAD65 promoter. The Imp neurons were observed as clusters of densely packed cells or as thin strands of cells present between the BL and Ce nuclei. Pairs of recorded neurons were included in the study only if their somata were detected by light microscopy within the intermediate capsule (see Supplemental Fig. 1). Presynaptic action currents resulted in failures and unitary inhibitory postsynaptic currents (uIPSCs) in neurons recorded at $V_{\mathrm{H}} = -50$ mV. Out of 635 recorded cell pairs, 14% of them were synaptically coupled and in one case a bidirectional connection was detected. Action currents were elicited in the presynaptic neurons at different frequencies ranging from 0.1 to 10 Hz, in slices from animals of similar age ($P > 0.05$, Kruskal–Wallis test). We observed that the occurrence of uIPSCs, as opposed to synaptic failures, in approximately 60% of the pairs was frequency dependent. For each cell pair, the success rate of events was plotted *versus* the frequencies of stimulation and fitted by a non-linear regression analysis using a logarithmic equation (Fig. 1). When the fit was significant, we defined a connection as 'facilitating' or 'depressing' ($P < 0.05$, r^2 was 0.86 ± 0.02 and 0.84 ± 0.01, respectively), whereas when it was not significant ($P > 0.05$, r^2 was 0.34 ± 0.04) the synaptic connection was classified as 'constant'. In the facilitating synaptic connections ($n = 25$), the occurrence of uIPSCs was lower at low frequency than at higher frequencies of stimulation (Fig. 1*A*). In the depressing connections ($n = 29$) uIPSCs were reliably evoked at low frequency and gradually their occurrence decreased at higher frequency of stimulation (Fig. 1*B*). In the constant connections ($n = 34$) the occurrence of uIPSCs was frequency independent (Fig. 1*C*). The changes in uIPSCs were short-term, since the success rate of uIPSCs returned to control values when the frequency of stimulation was switched back to 0.1 Hz (Wilcoxon signed ranks test, $P > 0.05$ for each comparison). The success rate of the uIPSCs became frequency independent when facilitating and depressing responses were pooled and averaged (Supplemental Fig. 2). Further experiments indicated that the uIPSCs evoked by presynaptic action currents at 0.1 Hz were stable over 40–80 min of recording ($n = 4$) and were entirely mediated by $\mathrm{GABA_A}$ receptors, since they were reversibly abolished by the application of 2 μM gabazine ($n = 3$, Supplemental Fig. 3).

We also analysed the amplitude and kinetic parameters of the uIPSCs evoked at 0.1–10 Hz. The peak amplitude of the uIPSCs excluding failures had a tendency to increase for facilitating connections and to decrease for depressing and constant connections, as the stimulation frequency was increased. However, these changes reached statistical significance only for the peak amplitude of uIPSCs of the depressing connections, which was significantly reduced at 10 Hz compared to 0.1 and 0.3 Hz ($P < 0.05$, $n = 28$, Kruskal–Wallis test, Fig. 2*A*). Moreover, the peak amplitude of uIPSCs including failures significantly increased or decreased, in a frequency-dependent manner, for facilitating and depressing, respectively, but not in constant connections (Fig. 2*B*, $n = 22$, $n = 28$ and $n = 32$, Kruskal–Wallis test, for *P*-values see the figure legend). Thus, presynaptic factors are likely to be involved in most of the facilitating connections, whereas postsynaptic changes could also underlie the synaptic dynamics of the depressing connections. The decay time constant and the rise time of the uIPSCs evoked at different frequencies of stimulation within each group of pairs were not significantly different ($P > 0.05$, Kruskal–Wallis test, n range = 17–32, Fig. 2*C* and Table 1). Furthermore, the peak amplitudes without failures, decay time constant or rise time of the uIPSCs evoked at 0.1–10 Hz were not significantly different among facilitating, depressing or constant connections ($P > 0.05$, Kruskal–Wallis test, n range = 17–32, Fig. 2*A* and Table 1), except for the peak amplitude of depressing *versus* facilitating or constant connections evoked at 10 Hz. Histograms summarizing basic parameters of uIPSCs pooled from the three groups of cell pairs are shown in Supplemental Fig. 4.

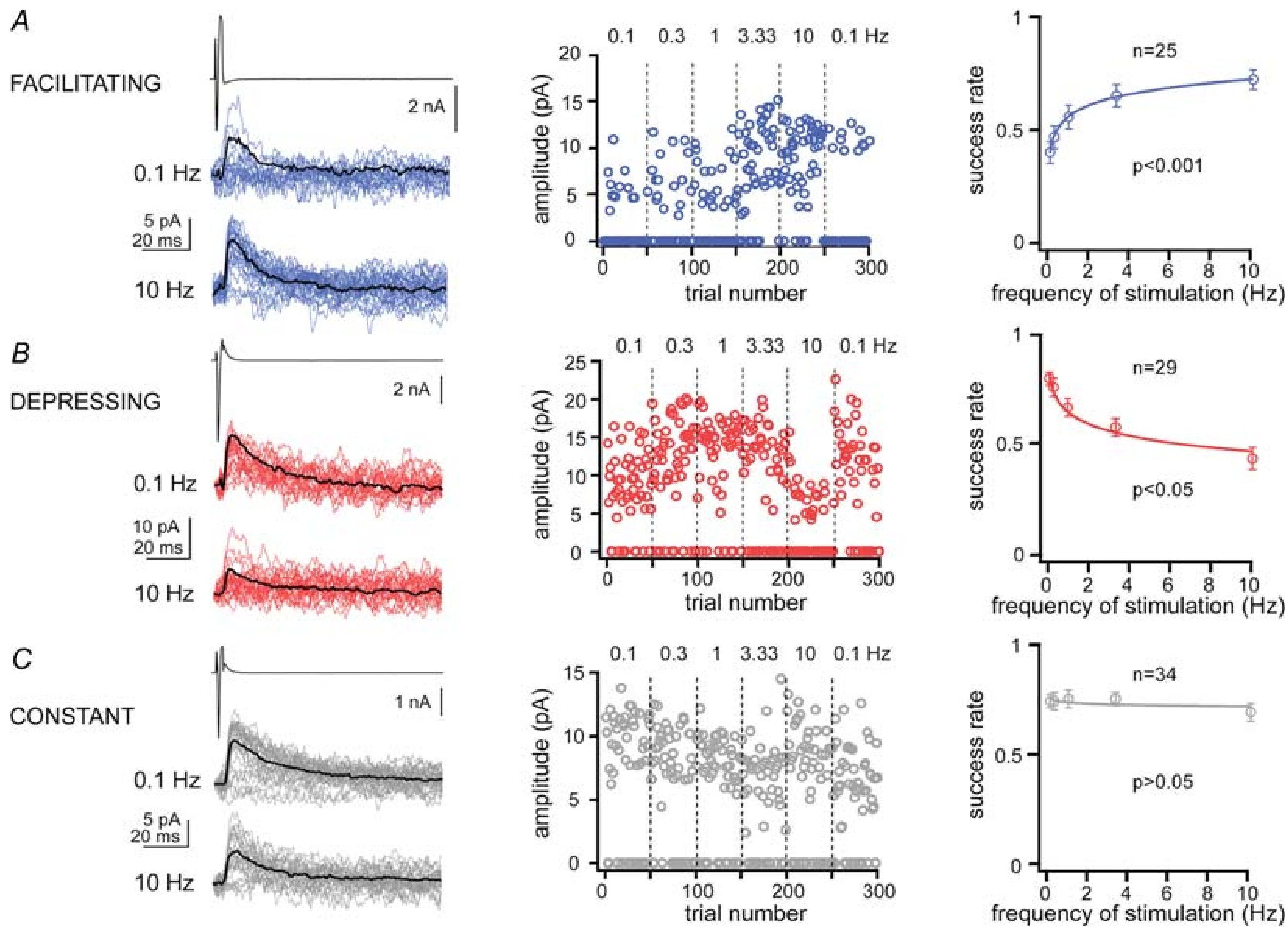

Figure 1. Dynamics of synaptic transmission between Imp cell pairs

For each panel, on the left, upper traces are action currents, and middle and lower traces are postsynaptic uIPSCs, evoked at 0.1 and 10 Hz, respectively, in facilitating (*A*), depressing (*B*) and constant (*C*) connections. Black traces are averages of uIPSCs without failures. Middle graphs, trial number versus peak amplitude of the uIPSCs for the experiments shown on the left. Numbers above the graphs are the frequencies of stimulation used (range: 0.1–10 Hz). Note that changes in success rate and amplitude (depressing) during high frequency stimulation reversed back to control values with 0.1 Hz stimulation. Right plots, nonlinear regression analysis of pooled data using a logarithmic equation to fit success rates of events, as opposed to failures, versus frequencies of stimulation; $P < 0.05$ indicates significant fit, and thus frequency dependency, whereas $P > 0.05$ indicates frequency independency; *n*, denotes the number of cell pairs for each group.

Presynaptic factors mainly determine synaptic heterogeneity in Imp neurons

The observed frequency-dependent changes in the number of failures strongly suggest a modification in the presynaptic release of transmitter (Dobrunz & Stevens, 1997). If presynaptic factors determine the changes observed, then the release probability of cell pairs showing depressing or facilitating responses should be different (Debanne *et al.* 1996; Dobrunz & Stevens, 1997). This was tested by analysing the paired-pulse ratio (PPR) of the synaptic responses elicited by two presynaptic action currents evoked at 50 ms interstimulus interval (ISI), including the synaptic failures. Facilitating connections showed paired-pulse facilitation (1.19 ± 0.15, $n = 9$), whereas depressing connections displayed paired-pulse depression (0.66 ± 0.06, $n = 6$). The PPR was significantly higher in facilitating compared to depressing connections ($P < 0.01$, Kruskal–Wallis test, Fig. 3*A*). The PPR was also analysed as potency ratio, namely the ratio of successes without failures. These values were 1 ± 0.07 for facilitating and 0.73 ± 0.07 for depressing connections

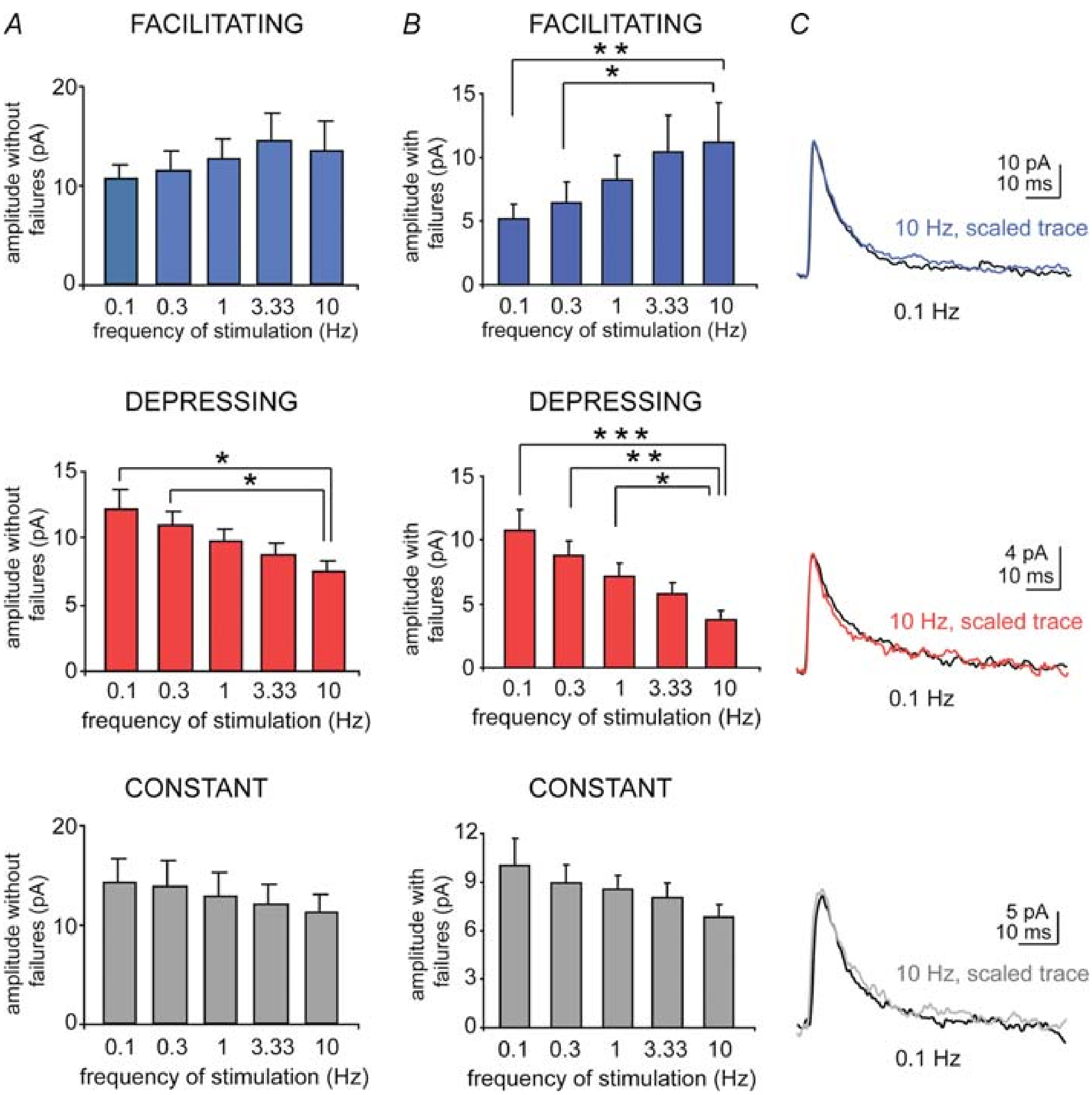

Figure 2. Effects of the frequency of stimulation on amplitude, rise time and decay time of uIPSCs
A, histograms refer to the mean of amplitude of uIPSCs calculated without including failures (Kruskal–Wallis test, $P > 0.05$ for all comparisons except $^*P < 0.05$). Note that the 10 Hz-evoked uIPSC amplitude of the depressing group (middle) is significantly different from that of constant (bottom) and facilitating (top) groups. *B*, histograms show the mean amplitude of uIPSCs including failures (Kruskal–Wallis test, $^*P < 0.05$, $^{**}P < 0.01$, $^{***}P < 0.005$, respectively). *C*, traces: scaled average uIPSCs (50 sweeps) evoked at 10 Hz (coloured traces) and 0.1 Hz (black traces), superimposed.

Table 1. Synaptic responses of Imp neurons

	Rise time (ms)						Decay time (ms)					
Frequency (Hz)	Facilitating	(*n*)	Depressing	(*n*)	Constant	(*n*)	Facilitating	(*n*)	Depressing	(*n*)	Constant	(*n*)
0.1	1.4 ± 0.1	19	1.2 ± 0.1	27	1.3 ± 0.1	32	13 ± 1	19	13.8 ± 1.1	27	14.6 ± 0.8	32
0.3	1.3 ± 0.1	19	1.2 ± 0.09	25	1.4 ± 0.1	31	14.5 ± 1.1	18	13 ± 1	25	14.6 ± 0.8	30
1	1.2 ± 0.08	21	1.2 ± 0.16	28	1.3 ± 0.09	30	14 ± 0.8	21	13.5 ± 0.82	24	14.3 ± 0.9	29
3.33	1.3 ± 0.08	21	1.3 ± 0.13	23	1.3 ± 0.09	29	14.6 ± 0.7	19	14.7 ± 1.2	22	13.7 ± 1.8	26
10	1.3 ± 0.09	23	1.5 ± 0.13	19	1.5 ± 0.09	30	14.2 ± 0.7	23	14.3 ± 0.87	17	13.6 ± 0.7	29

Average values ± S.E.M. and the number of recordings (*n*) are given. Statistics were computed using Kruskal–Wallis and Dunn's posthoc tests.

($P < 0.05$, Kruskal–Wallis test), confirming the changes of the uIPSCs peak amplitude excluding failures as a function of 0.1–10 Hz stimulations.

If a low release probability determines the high percentage of failures elicited by low frequency of stimulation in the facilitating type of connections, then increasing the concentration of Ca^{2+} in the ACSF should decrease the failure rate (Debanne *et al.* 1996; Jiang *et al.* 2000) changing the synaptic phenotype. Indeed, this is what we observed when the concentration of Ca^{2+} in the ACSF was raised from 2.5 mM to 5 mM (Fig. 3*B*). The success rate of uIPSCs was significantly enhanced when presynaptic action currents were evoked at 0.1 and 0.3 Hz ($P < 0.05$, paired *t* test, $n = 5$ and 4, respectively, Fig. 3*B*). Conversely, the amplitude of the uIPSCs evoked at any frequency of stimulation, calculated without failures, remained unchanged when Ca^{2+} was raised to 5 mM (Fig. 3*B*, $P > 0.05$, paired *t* test), confirming that one releasing site was mostly involved in this type of synaptic connections (Silver *et al.* 1996).

Target-cell does not determine the type of synaptic connections

The previous findings demonstrated that the short-term plasticity we observed was mainly determined by presynaptic mechanisms. This raises the question: do all terminals of the same axon form the same type of connections or do they form target-cell specific synaptic connections (Toth & McBain, 2000)? To answer this question, we performed sequential paired recordings, so that a protocol of stimulation at 0.1–10 Hz was performed on a cell pair, and then the same protocol was repeated in another cell pair in which the presynaptic neuron remained the same as in the first cell pair (Fig. 4*A*). Due to the low probability to detect synaptically coupled pairs, it was possible to obtain a total of $n = 9$ successful sequential recordings of connected cell pairs. This approach showed that the type of synaptic connections did not differ between the two sequential cell pairs, namely if the connection between the first cell pair was depressing, the connection between the second cell pair was also depressing. The same applied for the facilitating and constant types of connections (facilitating, $n = 3$, depressing, $n = 3$, constant, $n = 3$ sequential paired recordings, Fig. 4*B*). Moreover, in a further sequential paired recording protocol, a presynaptic neuron, which gave rise to a facilitating connection was subsequently found to receive a constant connection from a different Imp cell (not shown).

These data are consistent with the idea that Imp neurons possess heterogeneous synapses and that the target cell does not influence the type of connections formed by the presynaptic neuron. However, these results do not exclude the possibility that the two sequentially recorded postsynaptic neurons belonged to different cell types. Therefore, in order to test further the target specificity within the Imp cell network, we performed another series of sequential paired recordings, so that a protocol of stimulation at 0.1–10 Hz was performed on a cell pair, and then the same protocol was repeated in another cell pair in which the presynaptic neuron was different from the first cell pair (Fig. 5*A*). We successfully performed this protocol in nine experiments. We observed that the same postsynaptic cell was targeted by both constant and facilitating inputs (Fig. 5*B*, $n = 3$), or that the postsynaptic neuron was contacted by a constant and then a depressing input (Fig. 5*B*, $n = 3$), or that the postsynaptic neuron was contacted by a depressing and a facilitating input (Fig. 5*B*, $n = 3$). Thus, the presynaptic, but not the target, cell determines the heterogeneity of synaptic connections within the Imp cell network. Furthermore, these results also indicate that heterogeneous connections converge onto the same postsynaptic cell.

$GABA_B$ and CB_1 receptors do not tonically modulate the synaptic transmission between Imp neurons

A wealth of data shows that the presynaptic cannabinoid receptor type 1 (CB1) tonically inhibits the release of GABA from specific types of interneurons (Losonczy *et al.* 2004; Chevaleyre *et al.* 2006). To test whether a similar mechanism determined the high proportion of synaptic failures occurring at low frequency of stimulation in facilitating connections, the frequency-dependent protocol was performed before and 10–15 min after the application of the selective CB1 antagonist, AM251 (10 μM). In all experiments performed, AM251 did not change the proportion of failures or the peak amplitude of the uIPSCs elicited by each frequency of stimulation, and thus did not change the type of connections ($P > 0.05$, paired t test, $n = 5$, Supplemental Fig. 5*a*). A similar

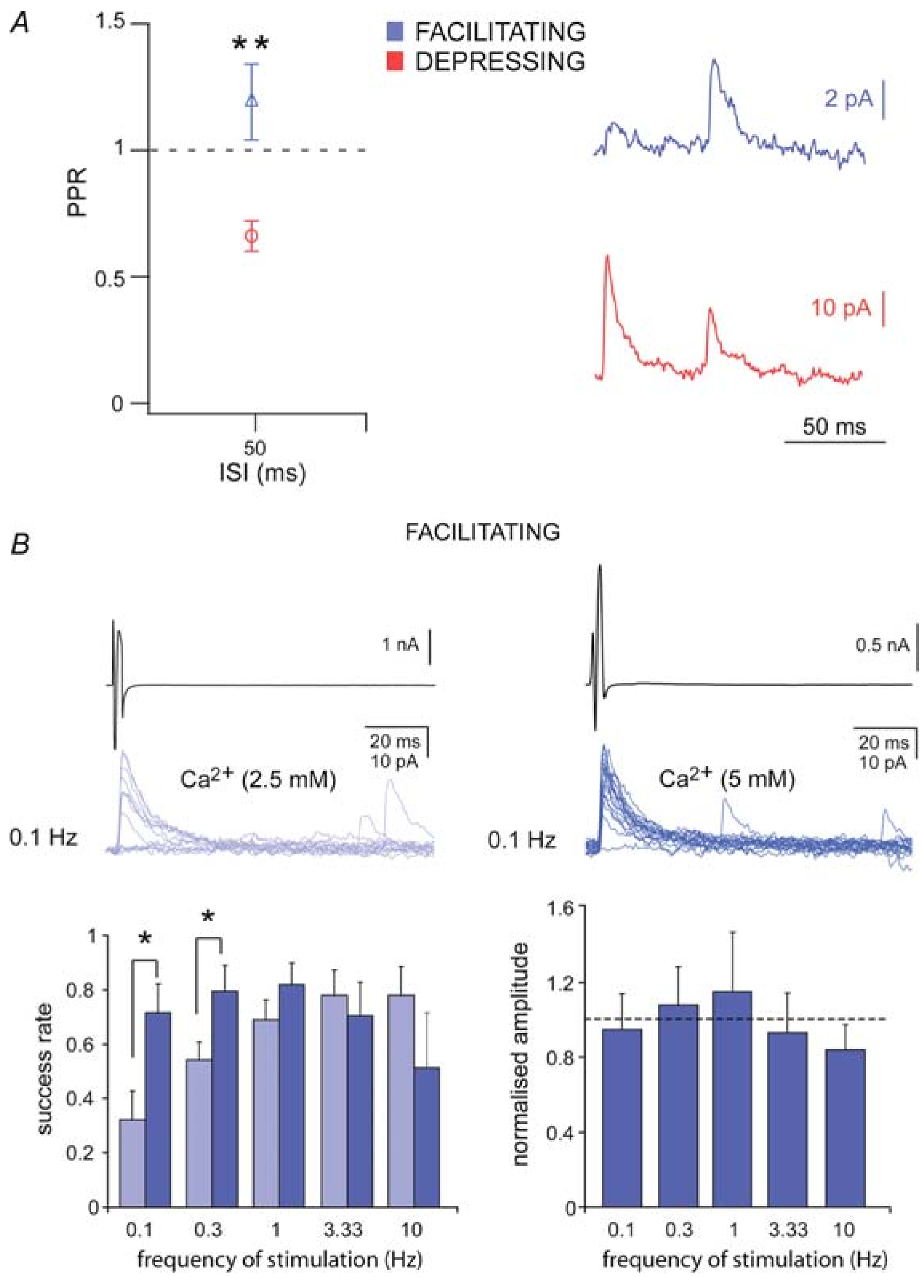

Figure 3. Presynaptic factors determine facilitating synaptic connections
A, paired pulse ratio (PPR) plotted against interstimulus interval (ISI) for facilitating and depressing Imp connected pairs (Kruskall-Wallis test, $^{**}P < 0.01$). Averaged traces (middle, from 30 sweeps, including failures) showing uIPSCs evoked by two action currents in the presynaptic Imp neurons, separated by 50 ms ISI. *B*, uIPSCs evoked by presynaptic action currents (black trace, 0.1 Hz) in control ACSF (2.5 mM Ca^{2+} and 2 mM Mg^{2+}, grey traces) and in ACSF containing 5 mM Ca^{2+} and 2 mM Mg^{2+} (blue traces) to increase the release probability. Normalized success rate (middle) plotted against frequency of stimulation in control ACSF (grey bars) and after the increase of Ca^{2+}/Mg^{2+} ratio (blue bars) in facilitating synaptic connections. Normalized amplitude of uIPSCs, calculated without failures (right), obtained in ACSF with 5 mM Ca^{2+} plotted against the frequency of stimulation. The peak amplitude is normalized to the uIPSCs obtained in control ACSF for each frequency ($^{*}P < 0.05$, paired t test).

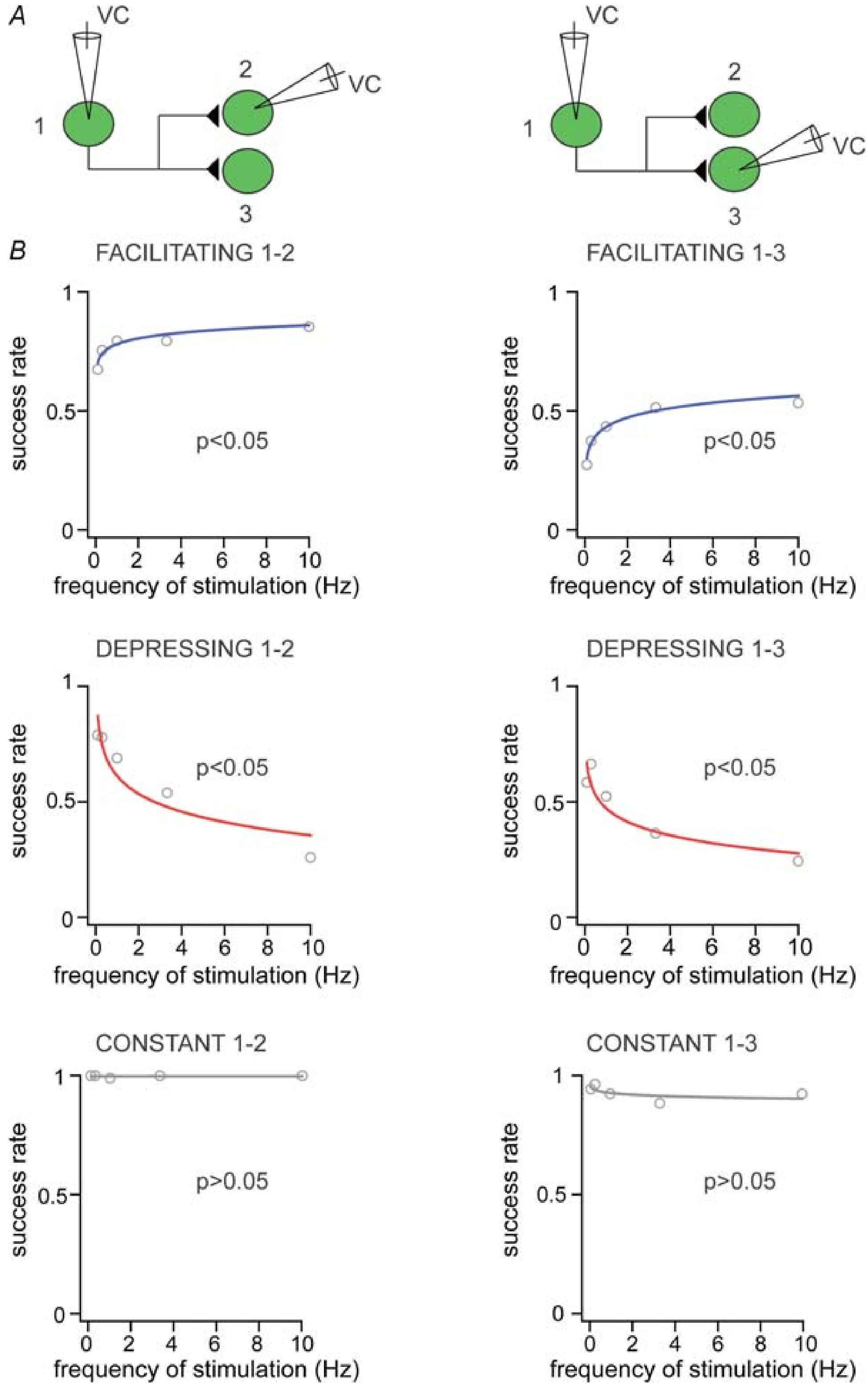

Figure 4. Target cells do not influence the type of connections amongst Imp neurons
A, experimental design of sequential pair recordings (1–2 and 1–3) of three Imp neurons synaptically coupled. *B*, success rate of the events plotted against frequency of stimulation for facilitating, depressing and constant cell pairs for the first (1–2, left) and second (1–3, right) sequence; $P < 0.05$ indicates significant fit, and thus frequency dependency, whereas $P > 0.05$ indicates frequency independency. VC, voltage clamp.

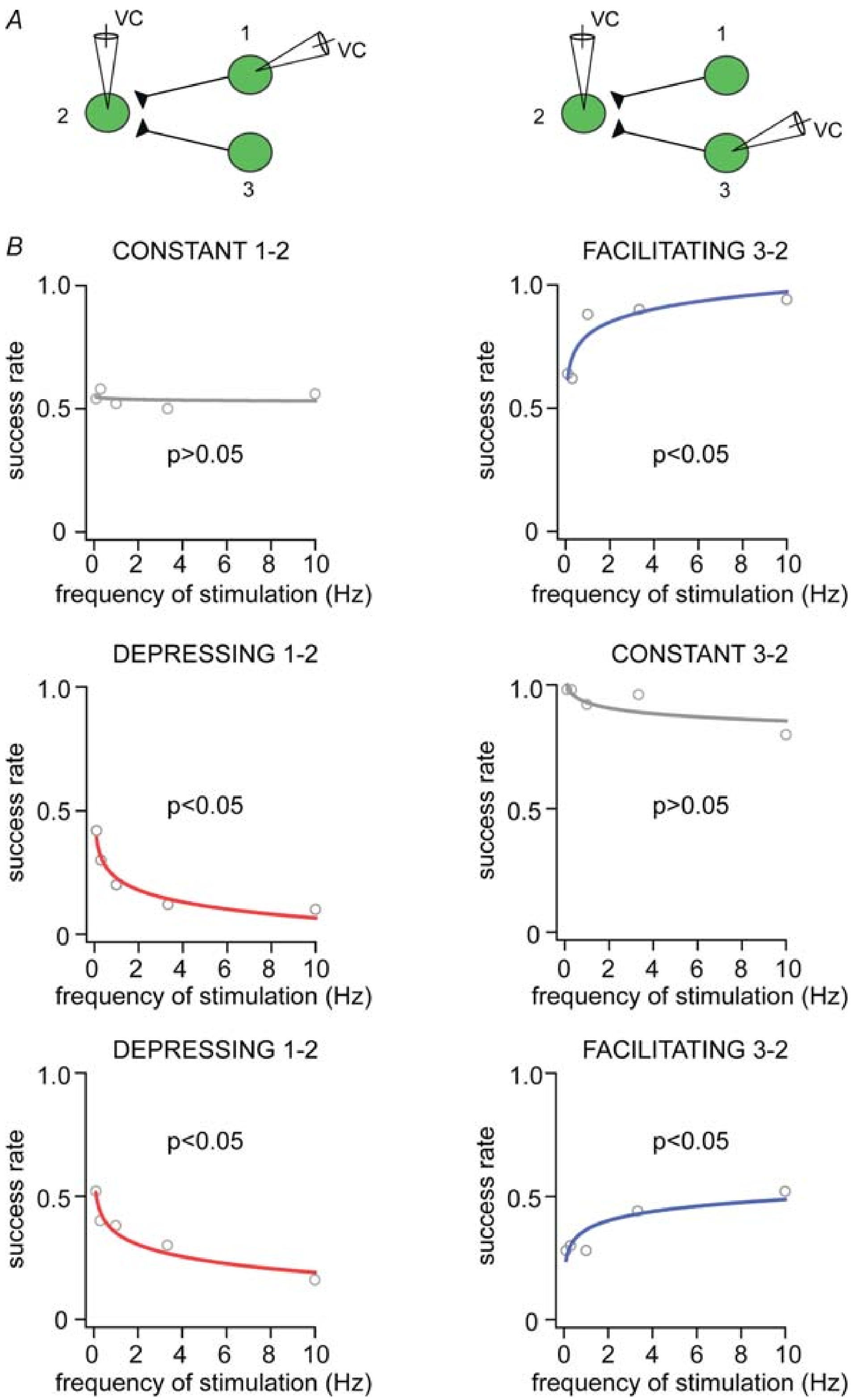

Figure 5. Different inhibitory inputs target the same Imp neuron
A, experimental design of sequential pair recordings (1–2 and 3–2) of three Imp neurons synaptically coupled. *B*, success rate of the events plotted against frequency of stimulation for the first (1–2, left) and second (3–2, right) sequence; namely constant and then facilitating connections (upper plots), depressing and then constant connections (middle plots), depressing and then facilitating connections (lower plots), $P < 0.05$ indicates significant fit, and thus frequency dependency, whereas $P > 0.05$ indicates frequency independency. VC, voltage clamp.

Table 2. Passive and active membrane properties of Imp neurons

	Presynaptic cell						Postsynaptic cell					
Parameter	Facilitating	(*n*)	Depressing	(*n*)	Constant	(*n*)	Facilitating	(*n*)	Depressing	(*n*)	Constant	(*n*)
RMP (mV)	-84.9 ± 1.8	16	-82.7 ± 2.1	20	-84.3 ± 1.4	24	-87.5 ± 1.9	15	-92 ± 1.8	21	-87.8 ± 1.5	24
R_{in} (MΩ)	485.5 ± 63	10	658.6 ± 95	14	419.7 ± 66	8	517 ± 93	13	557 ± 80	15	527 ± 85	15
Membrane τ (ms)	24.5 ± 2.4	10	27.1 ± 2	14	25.9 ± 3.7	11	25.6 ± 3.1	13	26 ± 1.5	15	32.4 ± 2.3	13
C_m (nF)	0.06 ± 0.01	10	0.05 ± 0.01	14	0.07 ± 0.01	10	0.07 ± 0.01	12	0.06 ± 0.01	15	0.08 ± 0.01	13
AHP (mV)	-9.7 ± 1	10	-10.8 ± 0.8	13	-10.9 ± 1.1	11	-9.7 ± 0.7	13	-12 ± 1.5	13	-8.7 ± 1.2	15
AP amplitude (mV)	73.4 ± 3	9	78 ± 2.4	13	76.2 ± 2.7	11	76.1 ± 3	13	81.5 ± 2	13	79.7 ± 2	11
AP width (ms)	0.8 ± 0.06	8	0.66 ± 0.03	13	0.61 ± 0.06	11	0.71 ± 0.04	13	0.62 ± 0.06	13	0.78 ± 0.04	11
Sag ratio	0.92 ± 0.01	9	0.89 ± 0.01	13	0.94 ± 0.01	11	0.91 ± 0.02	14	0.92 ± 0.03	14	0.91 ± 0.03	15
Adaptation index	0.78 ± 0.07	8	0.81 ± 0.04	12	0.8 ± 0.05	10	0.88 ± 0.05	13	0.74 ± 0.05	11	0.86 ± 0.04	13
Max. firing (Hz)	27.6 ± 2.9	7	30.3 ± 4.1	12	34.6 ± 5.5	9	28.8 ± 2.6	12	30.2 ± 4.3	12	29.3 ± 1.9	12

Average values ± S.E.M. and the number of recordings (n) are given. Statistics were computed using Kruskal–Wallis and Dunn's posthoc tests. RMP = resting membrane potential; R_{in} = input resistance; C_m = membrane capacitance; AHP = afterhyperpolarization; AP = action potential; Max. firing = maximal firing rate

protocol was also applied to test a possible modulatory role of presynaptic $GABA_B$ receptors at depressing cell pairs (Price *et al.* 2005). Application of the $GABA_B$ receptor antagonist CGP55845 (5 μM) did not significantly modify the proportion of failures or the peak amplitude of the uIPSCs elicited at each frequency of stimulation ($P > 0.05$, paired *t* test, $n = 4$, Supplemental Fig. 5*b*). As positive controls, we observed that AM251 (10 μM) and CGP55845 (5 μM) prevented the decrease of frequency and amplitude of spontaneous IPSCs (sIPSCs) elicited by bath application of the CB_1 or $GABA_B$ receptor agonists WIN55212-2 (5 μM) and baclofen (3 μM), respectively, in principal neurons of the BL nucleus, consistent with previous reports (Yamada *et al.* 1999; Marowsky *et al.* 2004). On average, the amplitude and frequency of sIPSCs recorded at $V_H = -60$ mV were 62.7 ± 2.9% and 66.4 ± 8.5% ($P < 0.05$, paired *t* test, $n = 4$) in the presence of WIN55212-2, and 109.2 ± 10.2% and 113.7 ± 4.3% ($P > 0.1$, paired *t* test, $n = 4$) after addition of AM251. Likewise, the amplitude and frequency of sIPSCs were 75.5 ± 5.9% and 69.7 ± 6.8% ($P < 0.05$, paired *t* test, $n = 4$) in the presence of baclofen, and 104.2 ± 5.9% and 94.6 ± 1.9% ($P > 0.05$, paired *t* test, $n = 4$) after addition of CGP55845.

Intrinsic membrane responses and anatomy of Imp neurons

To further assess whether the heterogeneous short-term plasticity observed is correlated to differences in Imp cells, additional analyses were performed. To this end we have studied several electrophysiological responses of the Imp connected neurons. We found that the passive and active membrane responses analysed were not significantly different between neurons forming facilitating, depressing or constant types of connections ($P > 0.05$, Kruskal–Wallis test, Table 2). A similar result was obtained comparing the same parameters of the pre- *versus* postsynaptic neurons within each group ($P > 0.05$, Mann–Whitney *U*-test).

We also performed anatomical analysis of the labelled Imp neurons, which revealed their characteristic bipolar shape with the primary dendrites orientated parallel to the intermediate capsule, in agreement with previous studies (Millhouse, 1986; Royer *et al.* 1999, 2000). The monosynaptically connected neurons in the three groups with different frequency-dependent synaptic strengths displayed several traits characteristic of each group. The frequency of neurons displaying a medium to high density of spines was different in pairs connected with facilitating synapses ($n = 17$) as compared to neurons in the constant ($n = 21$) and depressing ($n = 19$) groups (facilitating *versus* depressing, $P < 0.005$; facilitating *versus* constant, $P < 0.05$, Chi square test), which displayed a broader range of dendritic appearance in terms of density of spines (depressing *versus* constant, $P > 0.1$, Chi square test; see Supplemental Table 1). Conversely, the size of the somata of neurons in the three groups did not differ significantly ($P > 0.05$, Kruskal–Wallis test with Dunn's *post hoc* comparison, soma longest diameter: 18.3 ± 3.6 μm, facilitating; 18.3 ± 3.7 μm, depressing; 18.9 ± 3.4 μm, constant). These values were comparable to those previously reported for Imp neurons recorded in whole cell patch clamp (Royer *et al.* 2000). We have also analysed the somata based on size limits adopted from a previous Golgi-impregnation study of Ip neurons (Millhouse, 1986). The distribution in the different size classes did not appear to diverge amongst the three groups ($P > 0.05$, Chi square test). Marked differences were observed in the projections of the pre- and postsynaptic neurons composing the three functionally different groups of Imp cell pairs. In particular, in the group of depressing connected pairs, the presynaptic neuron gave rise to a primary axon that travelled through or around the

Ce nucleus toward the internal capsule (Fig. 6 and Supplemental Fig. 6) or in the stria terminalis. In some cases the axon appeared to target the intra-amygdaloid division of the bed nucleus of the stria terminalis. This pattern was not observed for axons of constant or facilitating connected neurons (Figs 7 and 8). Axonal collaterals of depressing connected pairs in several cases ran dorsally into the interstitial nucleus of the posterior limb of the anterior commissure (IPAC) or even entered the striatum. All three groups displayed conspicuous axonal projections coursing both ventrally and caudally in the intermediate capsule (Figs 6–8). The Ce nucleus was also found to be innervated by a number of collaterals, as previously reported (Millhouse, 1986; Pare & Smith, 1993*b*), which, however, originated from neurons in the constant or facilitating groups, but did not appear to derive from the depressing one. We also observed that the medial (Me) nucleus was an important target area for neurons of all three groups. Although axonal branches could be observed in the lateral (La) and BL nuclei, their distribution was very restricted, with little or no collaterals with few varicosities. For pairs with constant and facilitating connections it was often impossible to tell apart which axonal branches belonged to the pre- or the postsynaptic neuron due to the complex web of overlying collaterals.

Stability of the neuronal activity within the Imp network

Do uIPSCs, evoked by single presynaptic action potentials, affect the firing of the postsynaptic neurons? We have studied the effects of unitary inhibitory postsynaptic potentials (uIPSPs) evoked by presynaptic action potentials elicited at low frequency of stimulation (0.3 Hz, which displayed an optimal time window to perform the analysis in control and during the uIPSPs) on the firing of the postsynaptic cells recorded in current

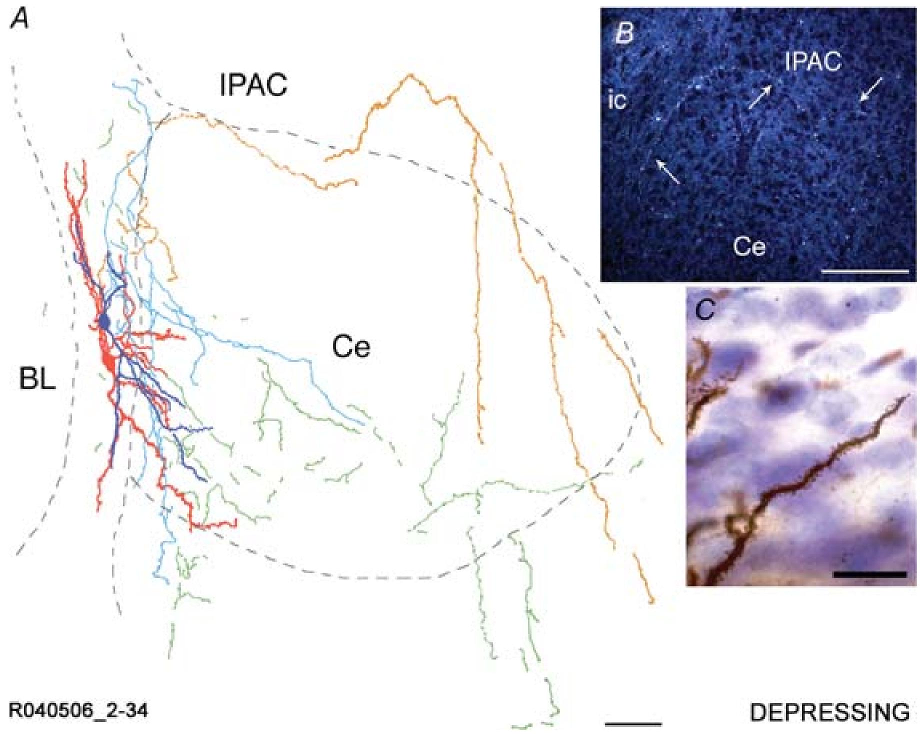

Figure 6. Reconstruction of an Imp cell pair synaptically coupled by a depressing type of connection
A representative cell pair is shown in *A* with soma and dendrites of the presynaptic Imp neuron drawn in red and its axonal arborizations drawn in orange. Soma and dendrites of the postsynaptic Imp neuron are drawn in dark blue, and its axonal arborizations are drawn in light blue. Portions of axons that could not be clearly associated with one of the two neurons are drawn in green. Note that the axon of the presynaptic neuron travels around the Ce nucleus. The somata are located in the intermediate capsule, their dendrites are running mainly in parallel to the intermediate capsule and just a small portion of the dendritic tree lies in the Ce nucleus. The delineation of the boundaries of the different amygdaloid nuclei is drawn from the section containing the somata. A dark-field micrograph of an additional cell pair (R122006 60–75) is shown in *B*. Note the axon running at the dorsal edge of the Ce nucleus towards the stria terminalis/internal capsule and back to the area of the intra-amygdaloid bed nucleus of the stria terminalis, indicated with arrows. A segment of a densely spiny dendrite belonging to the depressing cell pair R071406 1–19 is shown in *C*. BL, basolateral nucleus; Ce, central nucleus; ic, internal capsule; IPAC, interstitial nucleus of the posterior limb of the anterior commissure. Scale bars: *A*, 100 μm; *B*; 150 μm; *C*, 20 μm.

clamp mode. The membrane potential of the postsynaptic neurons was depolarized until spontaneous firing activity was elicited. The mean frequency of action potentials was 2.27 ± 0.54 Hz in facilitating, 3.36 ± 1.3 Hz in depressing and 1.46 ± 0.2 Hz in constant cell pairs, and these values were not significantly different ($P > 0.05$, Kruskal–Wallis test, $n = 5, 5, 8$, respectively). The uIPSPs did not modify the firing pattern of the postsynaptic cell for the facilitating connections, in which several synaptic failures occurred (Fig. 9*A*). Conversely, for both depressing and constant connections, the presence of the uIPSPs significantly inhibited the firing of the postsynaptic cells (Fig. 9*B*, *C*). The frequency of the action potentials during the control period and the 80 ms from the onset of the uIPSPs was 2.25 ± 0.42 Hz and 2.05 ± 0.86 Hz in the facilitating ($P > 0.05$, paired t test, $n = 5$), 3.65 ± 1.34 Hz

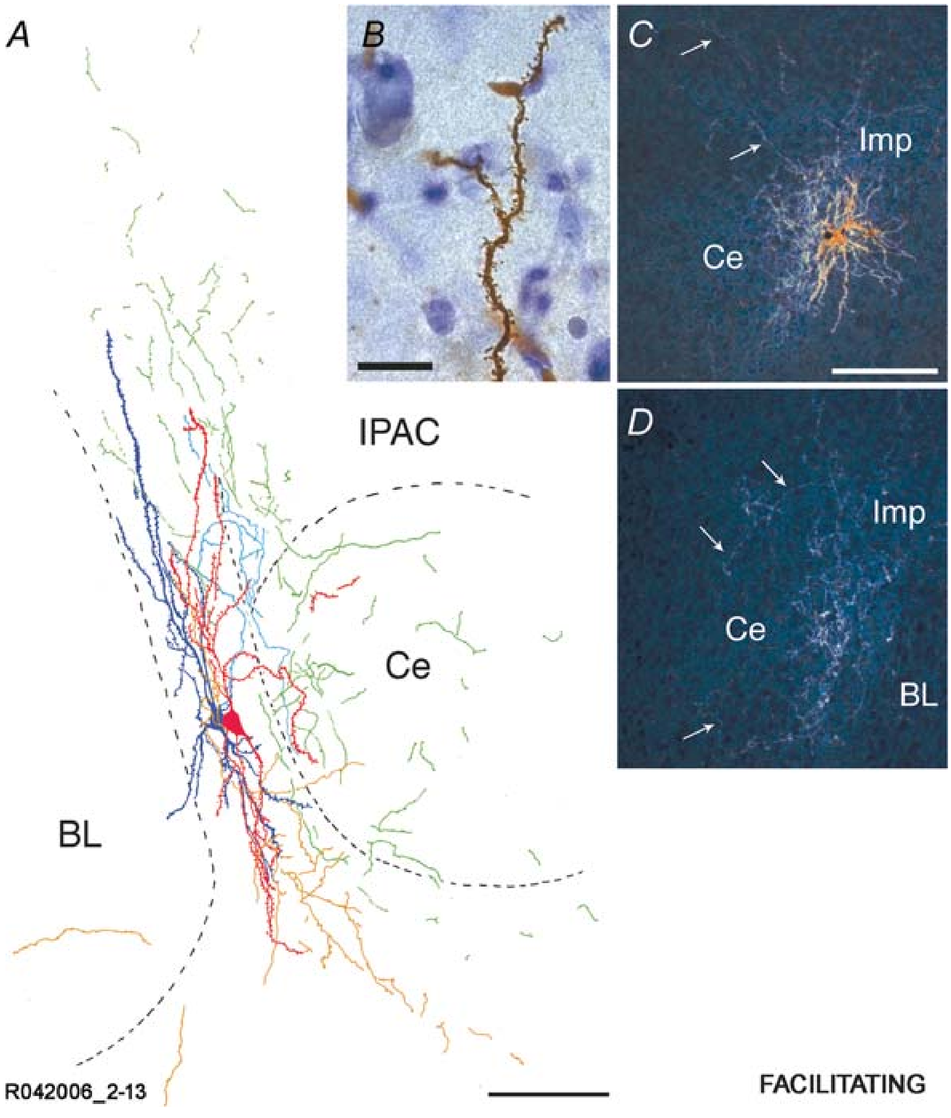

Figure 7. Reconstruction of an Imp cell pair synaptically coupled by a facilitating type of connection
A representative cell pair is shown in *A*. Soma and dendrites of the presynaptic Imp neuron are drawn in red, and axonal arborizations of this neuron are drawn in orange. Soma and dendrites of the postsynaptic Imp neuron are drawn in dark blue, and its axonal arborizations are drawn in light blue. Portions of axons that could not be clearly associated with one of the two neurons are drawn in green. Note that the somata are located in the intermediate capsule with their dendrites running in parallel with it, and the prominent innervation of the Ce nucleus. The delineation of the boundaries of the different amygdaloid nuclei is drawn from the section containing the somata. A high power bright light-field micrograph of a portion of a moderately spiny dendrite belonging to the facilitating cell pair R042006 2–13 is shown in *B*. Dark-field micrographs of consecutive sections of an additional facilitating pair (R120606 1–14) are shown in *C* and *D*. Axons innervating the Ce nucleus are indicated with arrows. BL, basolateral nucleus; Ce, central nucleus; Imp, medial paracapsular intercalated cells; IPAC, interstitial nucleus of the posterior limb of the anterior commissure. Scale bars: *A*, 100 μm; *B*; 15 μm; *C–D*, 150 μm.

and 1.15 ± 0.84 Hz in the depressing ($P < 0.05$, paired t test, $n = 5$) and 2 ± 0.24 Hz and 0.47 ± 0.15 Hz in the constant cell pairs ($P < 0.05$, Wilcoxon signed ranks test, $n = 8$). It is remarkable that uIPSPs were sufficient to modulate the firing of postsynaptic Imp neurons. However, constant or depressing, but not facilitating, connections effectively modulated the firing when the unitary events occurred at low frequency. These results

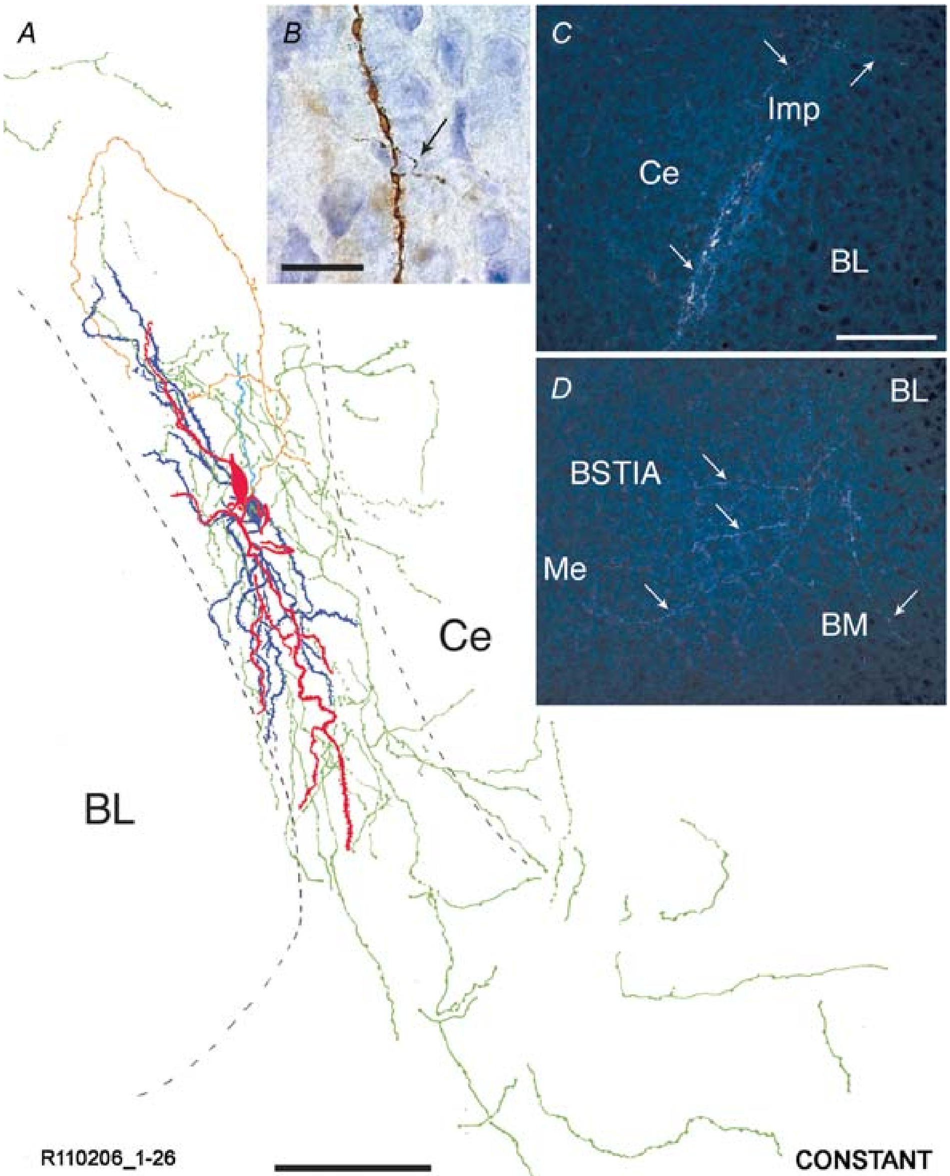

Figure 8. Reconstruction of an Imp cell pair synaptically coupled by a constant type of connection
A representative cell pair is shown in *A*. Soma and dendrites of the presynaptic Imp neuron are drawn in red, and axonal arborizations of this neuron are drawn in orange. Soma and dendrites of the postsynaptic Imp neuron are drawn in dark blue, and its axonal arborizations are drawn in light blue. Portions of axons that could not be clearly associated with one of the two neurons are drawn in green. Note that the somata and their dendritic tree are entirely restricted to the intermediate capsule. Their axons mainly course in this fibre bundle with extensions towards the Ce and Me nuclei. The delineation of the boundaries of the different amygdaloid nuclei is drawn from the section containing the somata. A high power bright light-field micrograph of a portion of a dendrite belonging to the constant pair R120806 1–20 is shown in *B*. Note that an axon (indicated by the arrow) intersects the dendrite possibly forming a synaptic contact. Dark-field micrographs of consecutive sections of a constant cell pair (R120806 1–20) are shown in *C* and *D*. Axons travelling along the intermediate caspule and heading towards the BM and Me nuclei are indicated with arrows. BL, basolateral nucleus; BM, basomedial nucleus; BSTIA, intra-amygdaloid bed nucleus of the stria terminalis; Ce, central nucleus; Imp, medial paracapsular intercalated cells; Me, medial nucleus. Scale bars: *A*, 100 μm; *B*, 20 μm; *C*–*D*, 150 μm.

suggest that presynaptic cells mediating facilitating and constant as well as facilitating and depressing connections have little effect onto the same postsynaptic neuron when they fire at low frequency, hence providing stability of the Imp network.

Discussion

We report here that amygdaloid Imp neurons are interconnected with variable synaptic strengths as a function of presynaptic activity. Such frequency-dependent heterogeneity appears to be particularly appropriate to maintain stability of the overall firing rate of the Imp neuronal population. Interestingly, a mechanism of activity-dependent modification of inhibitory synapses has been proposed as a model of rhythmic neural networks (Soto-Trevino *et al.* 2001). Theoretical considerations also indicate that stability of firing sequences contributes to the correct propagation of patterned activity from one group of neurons to the next, linked by feed-forward connections (Turrigiano & Nelson, 2004). The Imp neurons provide a feed-forward inhibitory gate for signals between the BL and Ce nuclei (Pare & Smith, 1993*b*; Royer *et al.* 1999; Marowsky *et al.* 2005), and from the infralimbic cortex to the Ce nucleus (Quirk *et al.* 2003; Berretta *et al.* 2005). Generally, feed-forward inhibition maintains timing across different cell populations, since it limits temporal summation of excitatory inputs (Pouille & Scanziani, 2001). Therefore, one possible function of Imp neurons is to modulate theta synchronization in amygdalo-hippocampal networks during fear memory consolidation and retrieval (Seidenbecher *et al.* 2003). Moreover, it has been proposed that when inputs from the thalamus to the lateral amygdala are strengthened, for example during a fear conditioned paradigm, the excitatory input onto Imp neurons with the soma placed more laterally is also strengthened (Royer *et al.* 2000; Pare *et al.* 2004). As a result, these Imp neurons inhibit other Imp neurons with the soma located more medially, disinhibiting neurons of the Ce nucleus and facilitating

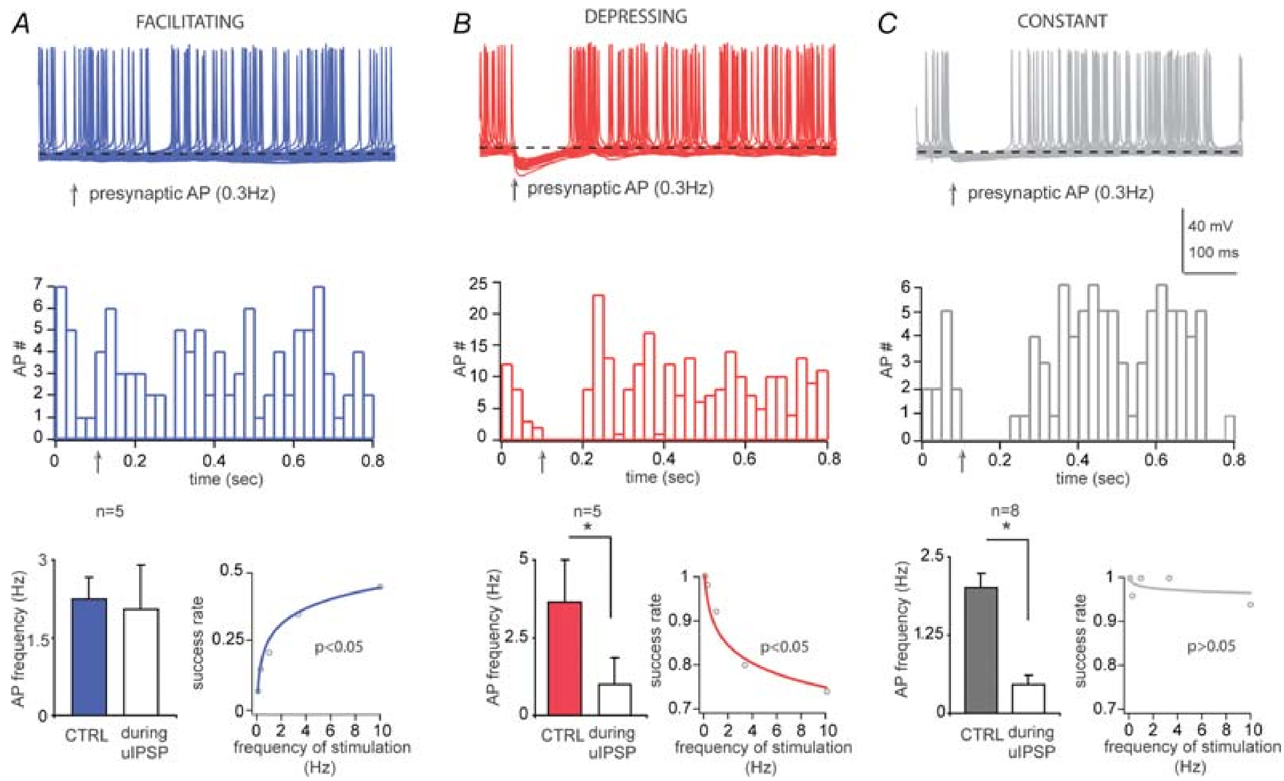

Figure 9. Depressing and constant, but not facilitating, synaptic transmission evoked at low frequency modulates the firing of postsynaptic Imp neurons

Upper traces, current-clamp recordings of postsynaptic Imp neurons superimposed (50 sweeps), in facilitating (*A*), depressing (*B*) and constant connections (*C*). The membrane potentials (dashed lines) were depolarized up to −57/−54 mV to elicit spontaneous firing activity. Middle plots, number of action potentials of the recordings shown above (bin size = 25 ms). Arrows indicate the time of occurrence of the presynaptic action potentials (APs). Lower histograms (left) show pooled data of frequency of action potentials in control (CTRL) and during the IPSPs (*$P < 0.05$, paired *t* test ($n = 5$) or Wilcoxon signed ranks test ($n = 8$)). Lower plots (right) illustrate nonlinear regression analysis testing the frequency dependency of the synaptic responses observed in the recordings shown above. In the plots, $P < 0.05$ indicates significant fit, and thus frequency dependency, whereas $P > 0.05$ indicates frequency independency.

their output toward the brainstem and the hypothalamus (Royer *et al.* 2000; Pare *et al.* 2004). Furthermore, the extinction of conditioned fear appears to involve the activity of the infralimbic cortex, which in turn inhibits the projecting neurons of the Ce nucleus (Quirk *et al.* 2003) via feed-forward activation of Imp neurons (Berretta *et al.* 2005). *In vivo* Imp neurons display much higher discharge rates than those observed in projection neurons of the BL or Ce nuclei (Pare & Gaudreau, 1996; Collins & Pare, 1999). It is worth to note that the frequency range we used to stimulate Imp neurons *in vitro* includes the frequency range of spontaneous action potentials detected *in vivo* (Collins & Pare, 1999).

The heterogeneous synaptic strengths we discovered should ensure a tight regulation of the modulation of tonic activity exerted by sensory and/or cortical information. Since the different synaptic strengths depend on the frequency of presynaptic activity, each type of synaptic connections should affect differently the output of the Imp network during sustained and oscillatory activity. The Imp cells seem to receive a mixture of facilitating, depressing and constant synapses. In a plausible scenario any change in firing rate will be compensated by opposite alterations in transmitter release probability at facilitating and depressing synapses converging onto the same cells. Further stability is ensured by the constant inhibitory connections that influence the activity of other Imp neurons in a frequency-independent manner, and by the similar proportion of the facilitating and depressing cell pairs. We can surmise that this strict control of the firing pattern of Imp neurons is needed to tune the gain of different excitatory inputs maintaining the Imp tonic inhibition constant, as it probably occurs during fear conditioning and extinction. The conservation of activity is an important property of neuronal networks, hence maintaining stability and ensuring the fidelity of the gain of transmission among neurons (Turrigiano & Nelson, 2004).

Our findings complement another kind of synaptic normalization that has been observed to operate at the level of the long-term effects of excitatory inputs onto Imp neurons (Royer & Pare, 2003). Specifically, activity-dependent potentiation or depression of excitatory inputs to Imp neurons was found to be accompanied by inverse modifications at heterosynaptic sites, and it has been proposed that this mechanism stabilizes the strength of overall excitability of Imp neurons (Royer & Pare, 2003). Thus, the network involving Imp neurons appears to require the maintenance of the total synaptic weight, both in terms of excitatory and inhibitory transmission. Redistribution of excitatory synaptic efficacy between neocortical neurons has been reported as another frequency-dependent mechanism to generate synaptic input diversity in neuronal networks (Markram & Tsodyks, 1996).

All Imp neurons that we have studied released GABA, confirming previous reports (Nitecka & Ben-Ari, 1987; Nitecka & Frotscher, 1989; McDonald & Augustine, 1993; Pare & Smith, 1993*a*; Royer *et al.* 1999; Marowsky *et al.* 2005), and the uIPSCs were entirely mediated by $GABA_A$ receptors. The available anatomical data regarding Imp neurons come from Golgi, intracellular neurobiotin injections and retrograde tract tracing studies performed in rats and cats (Kamal & Tombol, 1975; Millhouse, 1986; Pare & Smith, 1993*b*; Royer *et al.* 1999, 2000). Our findings not only corroborate these initial studies and extend them in the mouse but also provide a detailed analysis of the axonal outputs and dendritic features of Imp neurons. We confirm the view that the axons of Imp neurons give rise to numerous collaterals throughout their course in the intermediate capsule and provide an important innervation to the Ce and Me nuclei. We also demonstrate that the axonal patterns of these neurons are more elaborated, and hence not limited to intrinsic projections to the output nuclei of the amygdala. Axonal branches were observed to travel dorsally to the basal ganglia, or medially to the stria terminalis and/or internal capsule from where they could project to rostromedial forebrain areas or to the cortex. We also observed relevant differences in both the dendritic and axonal patterns of Imp neurons belonging to the facilitating, depressing or constant cell pairs, suggesting that they might represent different cell types. One of the most salient features found was that the parent axon of presynaptic neurons establishing depressing connections often coursed through or around the Ce nucleus avoiding innervating this nucleus to a significant extent. On the other hand, neurons forming facilitating connections gave rise to an extensive input to the Ce nucleus and did not appear to contribute extrinsic projections. Unlike the anatomical characteristics, none of the passive and active electrophysiological parameters studied differed among the three groups of Imp neurons defined by their frequency-dependent synaptic responses. Thus, the Imp neurons differ from interneurons of the BL complex, which can be divided into various subtypes based on their firing properties (Sosulina *et al.* 2006; Woodruff & Sah, 2007). Moreover, it was previously shown that Imp neurons of different clusters have directionally polarized connections, preferentially running in a latero-medial direction (Royer *et al.* 2000). We have not recorded from pairs of cells with the somata in different clusters, but only from cell pairs with the somata located in close proximity. In our experiments, we have not detected a preferential location of the soma of the pre- or the postsynaptic cell, in either a latero-medial or dorso-ventral axis that systematically increased the likelihood of synaptic coupling between two Imp neurons.

Our data indicate that the short-term plasticity observed in pairs of Imp neurons is mainly determined by presynaptic mechanisms. This conclusion was based on a number of lines of evidence: (1) the number of failures changed as a function of the frequency of synaptic stimulation (Dobrunz & Stevens, 1997); (2) depressing and facilitating cell pairs had different release probabilities, as assessed by a paired-pulse protocol (Debanne *et al.* 1996); (3) an increase in the concentration of extracellular Ca^{2+}, which enhances presynaptic release probability (Debanne *et al.* 1996; Jiang *et al.* 2000), significantly reduced the failure rates evoked by low frequency stimulation of the facilitating type of connections, so that it become constant; (4) the nature of the postsynaptic target did not influence the type of connections formed by the presynaptic neuron, thereby excluding a target-cell specificity (Toth & McBain, 2000) and different types of connections converged onto the same postsynaptic neuron. The result that heterogeneous synaptic inputs targeted the same postsynaptic cell further confirmed the absence of target specificity. We also found that the rise time and decay of uIPSCs were not affected by different frequencies of stimulation. The peak amplitude of the uIPSCs, measured with or without failures, significantly decreased as the frequency of stimulation increased, in the depressing type of connections, indicating that post-synaptic factors could also contribute to the plastic changes observed (Rozov & Burnashev, 1999) or that multiple connections fail gradually. Conversely, an opposite trend, which becomes significant only when failures were included in the analysis, was observed in the facilitating cell pairs. Noteworthy, in these synaptic connections, the increase of extracellular Ca^{2+} did not change the uIPSCs amplitude but only the success rates, further suggesting that only one releasing site was mostly involved (Silver *et al.* 1996).

We also tested whether CB1 receptors, which have been shown to tonically depress the release of GABA at other synapses (Losonczy *et al.* 2004), could influence the failure rate of the synaptic responses, but found no effect. This result agrees with an immunohistochemical study showing that CB1 receptors are undetectable in the intermediate capsule in contrast to other amygdaloid nuclei (Katona *et al.* 2001), and indicates that their negative result was not due to a low sensitivity of the antibody used. Our results also ruled out a tonic influence by presynaptic $GABA_B$ receptors, which has been documented at other synapses (Price *et al.* 2005).

In conclusion, our data reveal unexpected heterogeneity in neurotransmitter release probability and in dendritic and axonal patterns of Imp neurons. We propose that this variability has biological significance (Soltesz, 2006) and generates stability of firing within the Imp cell population.

References

Abbott LF & Nelson SB (2000). Synaptic plasticity: taming the beast. *Nat Neurosci* **3** (Suppl.), 1178–1183.

Alheid GF, de Olmos JS & Beltramino CA (1994). Amygdala and extended amygdala. In *The Rat Nervous System*, 2nd edn (ed. Paxinos G), pp. 495–578. Academic Press, Inc, San Diego, CA, USA.

Bekkers JM, Richerson GB & Stevens CF (1990). Origin of variability in quantal size in cultured hippocampal neurons and hippocampal slices. *Proc Natl Acad Sci U S A* **87**, 5359–5362.

Berretta S, Pantazopoulos H, Caldera M, Pantazopoulos P & Pare D (2005). Infralimbic cortex activation increases c-Fos expression in intercalated neurons of the amygdala. *Neuroscience* **132**, 943–953.

Borowski TB & Kokkinidis L (1998). The effects of cocaine, amphetamine, and the dopamine D1 receptor agonist SKF 38393 on fear extinction as measured with potentiated startle: implications for psychomotor stimulant psychosis. *Behav Neurosci* **112**, 952–965.

Capogna M, Volynski KE, Emptage NJ & Ushkaryov YA (2003). The α-latrotoxin mutant LTXN4C enhances spontaneous and evoked transmitter release in CA3 pyramidal neurons. *J Neurosci* **23**, 4044–4053.

Chevaleyre V, Takahashi KA & Castillo PE (2006). Endocannabinoid-mediated synaptic plasticity in the CNS. *Annu Rev Neurosci* **29**, 37–76.

Collins DR & Pare D (1999). Spontaneous and evoked activity of intercalated amygdala neurons. *Eur J Neurosci* **11**, 3441–3448.

Debanne D, Guerineau NC, Gahwiler BH & Thompson SM (1996). Paired-pulse facilitation and depression at unitary synapses in rat hippocampus: quantal fluctuation affects subsequent release. *J Physiol* **491**, 163–176.

Dobrunz LE & Stevens CF (1997). Heterogeneity of release probability, facilitation, and depletion at central synapses. *Neuron* **18**, 995–1008.

Ferraguti F, Cobden P, Pollard M, Cope D, Shigemoto R, Watanabe M & Somogyi P (2004). Immunolocalization of metabotropic glutamate receptor 1α (mGluR1α) in distinct classes of interneuron in the CA1 region of the rat hippocampus. *Hippocampus* **14**, 193–215.

Fuxe K, Jacobsen KX, Hoistad M, Tinner B, Jansson A, Staines WA & Agnati LF (2003). The dopamine D1 receptor-rich main and paracapsular intercalated nerve cell groups of the rat amygdala: relationship to the dopamine innervation. *Neuroscience* **119**, 733–746.

Jiang L, Sun S, Nedergaard M & Kang J (2000). Paired-pulse modulation at individual GABAergic synapses in rat hippocampus. *J Physiol* **523**, 425–439.

Kamal AM & Tombol T (1975). Golgi studies on the amygdaloid nuclei of the cat. *J Hirnforsch* **16**, 175–201.

Katona I, Rancz EA, Acsady L, Ledent C, Mackie K, Hajos N & Freund TF (2001). Distribution of CB1 cannabinoid receptors in the amygdala and their role in the control of GABAergic transmission. *J Neurosci* **21**, 9506–9518.

Larkman A, Stratford K & Jack J (1991). Quantal analysis of excitatory synaptic action and depression in hippocampal slices. *Nature* **350**, 344–347.

Lopez-Bendito G, Sturgess K, Erdelyi F, Szabo G, Molnar Z & Paulsen O (2004). Preferential origin and layer destination of GAD65-GFP cortical interneurons. *Cereb Cortex* **14**, 1122–1133.

Losonczy A, Biro AA & Nusser Z (2004). Persistently active cannabinoid receptors mute a subpopulation of hippocampal interneurons. *Proc Natl Acad Sci U S A* **101**, 1362–1367.

Markram H & Tsodyks M (1996). Redistribution of synaptic efficacy between neocortical pyramidal neurons. *Nature* **382**, 807–810.

Marowsky A, Fritschy JM & Vogt KE (2004). Functional mapping of GABA A receptor subtypes in the amygdala. *Eur J Neurosci* **20**, 1281–1289.

Marowsky A, Yanagawa Y, Obata K & Vogt KE (2005). A specialized subclass of interneurons mediates dopaminergic facilitation of amygdala function. *Neuron* **48**, 1025–1037.

McDonald AJ & Augustine JR (1993). Localization of GABA-like immunoreactivity in the monkey amygdala. *Neuroscience* **52**, 281–294.

Millhouse OE (1986). The intercalated cells of the amygdala. *J Comp Neurol* **247**, 246–271.

Nitecka L & Ben-Ari Y (1987). Distribution of GABA-like immunoreactivity in the rat amygdaloid complex. *J Comp Neurol* **266**, 45–55.

Nitecka L & Frotscher M (1989). Organization and synaptic interconnections of GABAergic and cholinergic elements in the rat amygdaloid nuclei: single- and double-immunolabeling studies. *J Comp Neurol* **279**, 470–488.

Pare D & Gaudreau H (1996). Projection cells and interneurons of the lateral and basolateral amygdala: distinct firing patterns and differential relation to theta and delta rhythms in conscious cats. *J Neurosci* **16**, 3334–3350.

Pare D, Quirk GJ & Ledoux JE (2004). New vistas on amygdala networks in conditioned fear. *J Neurophysiol* **92**, 1–9.

Pare D & Smith Y (1993*a*). Distribution of GABA immunoreactivity in the amygdaloid complex of the cat. *Neuroscience* **57**, 1061–1076.

Pare D & Smith Y (1993*b*). The intercalated cell masses project to the central and medial nuclei of the amygdala in cats. *Neuroscience* **57**, 1077–1090.

Pouille F & Scanziani M (2001). Enforcement of temporal fidelity in pyramidal cells by somatic feed-forward inhibition. *Science* **293**, 1159–1163.

Price CJ, Cauli B, Kovacs ER, Kulik A, Lambolez B, Shigemoto R & Capogna M (2005). Neurogliaform neurons form a novel inhibitory network in the hippocampal CA1 area. *J Neurosci* **25**, 6775–6786.

Quirk GJ, Likhtik E, Pelletier JG & Pare D (2003). Stimulation of medial prefrontal cortex decreases the responsiveness of central amygdala output neurons. *J Neurosci* **23**, 8800–8807.

Royer S, Martina M & Pare D (1999). An inhibitory interface gates impulse traffic between the input and output stations of the amygdala. *J Neurosci* **19**, 10575–10583.

Royer S, Martina M & Pare D (2000). Polarized synaptic interactions between intercalated neurons of the amygdala. *J Neurophysiol* **83**, 3509–3518.

Royer S & Pare D (2002). Bidirectional synaptic plasticity in intercalated amygdala neurons and the extinction of conditioned fear responses. *Neuroscience* **115**, 455–462.

Royer S & Pare D (2003). Conservation of total synaptic weight through balanced synaptic depression and potentiation. *Nature* **422**, 518–522.

Rozov A & Burnashev N (1999). Polyamine-dependent facilitation of postsynaptic AMPA receptors counteracts paired-pulse depression. *Nature* **401**, 594–598.

Seidenbecher T, Laxmi TR, Stork O & Pape HC (2003). Amygdalar and hippocampal theta rhythm synchronization during fear memory retrieval. *Science* **301**, 846–850.

Silver RA, Cull-Candy SG & Takahashi T (1996). Non-NMDA glutamate receptor occupancy and open probability at a rat cerebellar synapse with single and multiple release sites. *J Physiol* **494**, 231–250.

Soltesz I (2006). *Diversity in the Neuronal Machine*. Oxford University Press, Oxford, UK.

Sosulina L, Meis S, Seifert G, Steinhauser C & Pape HC (2006). Classification of projection neurons and interneurons in the rat lateral amygdala based upon cluster analysis. *Mol Cell Neurosci* **33**, 57–67.

Soto-Trevino C, Thoroughman KA, Marder E & Abbott LF (2001). Activity-dependent modification of inhibitory synapses in models of rhythmic neural networks. *Nat Neurosci* **4**, 297–303.

Thomson AM (2000). Facilitation, augmentation and potentiation at central synapses. *Trends Neurosci* **23**, 305–312.

Toth K & McBain CJ (2000). Target-specific expression of pre- and postsynaptic mechanisms. *J Physiol* **525**, 41–51.

Turrigiano GG & Nelson SB (2004). Homeostatic plasticity in the developing nervous system. *Nat Rev Neurosci* **5**, 97–107.

Woodruff AR & Sah P (2007). Networks of parvalbumin-positive interneurons in the basolateral amygdala. *J Neurosci* **27**, 553–563.

Yamada J, Saitow F, Satake S, Kiyohara T & Konishi S (1999). $GABA_B$ receptor-mediated presynaptic inhibition of glutamatergic and GABAergic transmission in the basolateral amygdala. *Neuropharmacology* **38**, 1743–1753.

Zucker RS & Regehr WG (2002). Short-term synaptic plasticity. *Annu Rev Physiol* **64**, 355–405.

Acknowledgements

This work was supported by the Medical Research Council, UK, by the Austrian Science Foundation FWF, grant No. P16720 to F.F., and by the Academic Research Collaboration Programme of the Federal Ministry for Education, Science and Culture and the British Council in Austria. R.G. was supported by Marie Curie Intra-European Fellowship within the 6th European Community Framework Programme. We thank Y. Dalezios, R. Hauer, B. Micklem, L. Norman and G. Schmid, for technical aid and expertise. We also thank P. Bolam, D. Elfant, T. Karayannis, Z. Nusser and P. Somogyi for comments on the manuscript.

Supplemental material

Online supplemental material for this paper can be accessed at: http://jp.physoc.org/cgi/content/full/jphysiol.2007.142570/DC1 and
http://www.blackwell-synergy.com/doi/suppl/10.1113/jphysiol.2007.142570